THE JOURNAL OF BIOLOGICAL CHEMISTRY VOL. 290, NO. 32, pp. 19823–19832, August 7, 2015

A Catalase-related Hemoprotein in Coral Is Specialized for Synthesis of Short-chain Aldehydes

*DISCOVERY OF P450-TYPE HYDROPEROXIDE LYASE ACTIVITY IN A CATALASE**

Received for publication, April 20, 2015, and in revised form, June 18, 2015 Published, JBC Papers in Press, June 22, 2015, DOI 10.1074/jbc.M115.660282

Tarvi Teder[‡§], Helike Lõhelaid[‡], William E. Boeglin[§], Wade M. Calcutt[¶], Alan R. Brash[§], and Nigulas Samel[‡1]

From the [‡]Department of Chemistry, Tallinn University of Technology, 12618 Tallinn, Estonia, [§]Department of Pharmacology and the Vanderbilt Institute of Chemical Biology, Vanderbilt University, Nashville, Tennessee 37232, and [¶]Department of Biochemistry, Vanderbilt University, Nashville, Tennessee

Background: Biosynthetic transformation of fatty acid peroxides commonly is catalyzed by cytochromes P450.
Results: A catalase-related hemoprotein in the coral *Capnella imbricata* converts 8*R*-hydroperoxy-eicosatetraenoic acid in a P450-type reaction to short-chain aldehydes.
Conclusion: A catalase-related hydroperoxide lyase is identified in Animalia.
Significance: The catalase-related hemoprotein has the catalytic competence of a P450.

In corals a catalase-lipoxygenase fusion protein transforms arachidonic acid to the allene oxide 8*R*,9-epoxy-5,9,11,14-eicosatetraenoic acid from which arise cyclopentenones such as the prostanoid-related clavulones. Recently we cloned two catalase-lipoxygenase fusion protein genes (*a* and *b*) from the coral *Capnella imbricata*, form *a* being an allene oxide synthase and form *b* giving uncharacterized polar products (Lõhelaid, H., Teder, T., Tõldsepp, K., Ekins, M., and Samel, N. (2014) *PloS ONE* 9, e89215). Here, using HPLC-UV, LC-MS, and NMR methods, we identify a novel activity of fusion protein b, establishing its role in cleaving the lipoxygenase product 8*R*-hydroperoxy-eicosatetraenoic acid into the short-chain aldehydes (5*Z*)-8-oxo-octenoic acid and (3*Z*,6*Z*)-dodecadienal; these primary products readily isomerize in an aqueous medium to the corresponding 6*E*- and 2*E*,6*Z* derivatives. This type of enzymatic cleavage, splitting the carbon chain within the conjugated diene of the hydroperoxide substrate, is known only in plant cytochrome P450 hydroperoxide lyases. In mechanistic studies using ^{18}O-labeled substrate and incubations in $H_2{}^{18}O$, we established synthesis of the C8-oxo acid and C12 aldehyde with the retention of the hydroperoxy oxygens, consistent with synthesis of a short-lived hemiacetal intermediate that breaks down spontaneously into the two aldehydes. Taken together with our initial studies indicating differing gene regulation of the allene oxide synthase and the newly identified catalase-related hydroperoxide lyase and given the role of aldehydes in plant defense, this work uncovers a potential pathway in coral stress signaling and a novel enzymatic activity in the animal kingdom.

Lipid mediator biosynthesis commonly involves the dioxygenation of a fatty acid followed by a cytochrome P450-catalyzed rearrangement of the resulting fatty acid peroxide in the next step of the pathway. In higher animals the cyclooxygenases are so coupled with thromboxane synthase (cytochrome P450 CYP5) or prostacyclin synthase (CYP8), thereby producing important mediators of vascular hemostasis (1). In plants, the pair of enzymes is usually a lipoxygenase (LOX),[2] forming a fatty acid hydroperoxide, and a member of the P450 CYP74 family with allene oxide synthase (AOS), divinyl ether synthase, or hydroperoxide lyase (HPL) activity (2, 3). These enzymes give rise to products including the plant hormone jasmonic acid via AOS and mediators of plant defense via the HPL (4). In fungi there are many examples of a single participating gene encoding a two-domain protein comprised of an N-terminal heme dioxygenase and a C-terminal cytochrome P450 (5–7). The resulting oxylipin products act as hormone-like signals modulating asexual and sexual spore development and in the production of toxins (7, 8).

Certain lower animals, best studied in corals, express a different type of fusion protein that consists of an N-terminal catalase-related hemoprotein coupled to a C-terminal LOX domain (9, 10). The prototypical enzyme of this type is the cAOS-LOX fusion protein, which dioxygenates arachidonic acid to an 8*R*-hydroperoxyeicosatetraenoic acid (8*R*-HpETE) intermediate followed by its conversion to an allene oxide by the cAOS domain (11). Although the plant AOS and cAOS catalyze similar reactions, the enzymes are structurally unrelated (12–14). The highly labile allene oxide products of both enzyme types readily break down to stable end products, α-ketol and cyclopentenone (6). Moreover, despite the structural relatedness to catalase, cAOS lacks the capability to catalyze the decomposition of hydrogen peroxide to water and molecular oxygen (14, 15).

* This work was supported, in whole or in part, by National Institutes of Health Grant GM-074888 (to A. R. B.). This work was also supported by the Institutional Research Funding IUT19–9 of the Estonian Ministry of Education and Research and the Estonian Science Foundation Grant 9410 (both to N. S.). The authors declare that they have no conflicts of interest with the contents of this article.

[1] To whom the correspondence may be addressed: Dept. of Chemistry, Tallinn University of Technology, 12618 Tallinn, Estonia. Tel.: 372-620-4376; Fax: 372-620-2828; E-mail: nigulas.samel@ttu.ee.

[2] The abbreviations used are: LOX, lipoxygenase; AA, arachidonic acid; AOS, allene oxide synthase; cAOS, catalase-related AOS; HPL, hydroperoxide lyase; cHPL, catalase-related HPL; 8*R*-H(p)ETE, 8*R*-hydro(pero)xyeicosatetraenoic acid; RP-HPLC, reversed phase HPLC; SP-HPLC, straight phase HPLC.

In our recent study of the soft coral *Capnella imbricata* we cloned two highly homologous catalase-lipoxygenase fusion proteins (designated **a** and **b**) with 88% of amino acid identity (16). Although the catalytically important amino acids of catalase-related and lipoxygenase domains were conserved, the biosynthesis with [1-^{14}C]arachidonic acid led to the formation of different products. Although fusion protein **a** catalyzed the formation of an α-ketol and cyclopentenone stable end products and thereby can be designated as a cAOS-LOX, incubation with fusion protein **b** gave rise to unknown polar compounds (16). Herein we present the identification of short-chain compounds formed by the catalase-related hemoprotein **b** and thereby characterize a fatty acid hydroperoxide lyase pathway in coral arachidonic acid metabolism.

Experimental Procedures

Materials—Arachidonic acid (AA) was purchased from Nu-Chek Prep Inc. (Elysian, MN). 8*R*-HpETE was synthesized using the *Plexaura homomalla* 8*R*-lipoxygenase domain of the cAOS-LOX fusion protein, expressed in *Escherichia coli* (11). The $^{18}O_2$-8*R*-HpETE was prepared from AA by *P. homomalla* 8*R*-LOX under an $^{18}O_2$ (Isotech (Miamisburg, OH)) atmosphere in a degassed buffer (50 mM Tris, pH 8.0). The ^{18}O-labeled water was purchased from the Mound Facility (Miamisburg, OH). Only HPLC grade solvents were used.

*Cloning and Expression of Fusion Protein **b** and the Catalase-related Domain*—The ORF of fusion protein **b** (GenBank™ accession number KF000374) with terminal NheI restriction sites and with an N-terminal His_6 tag was PCR-amplified from the fusion protein **b** construct (16) using forward (5′-ATTCATATGATGGTTTGGAAAAATTTTGGTTACG-3′) and reverse (5′-CAGCTAGCCTAGATTGCAGTTCCG-3′) primers. Subsequently, the ORF of the catalase-related domain with a stop codon and C-terminal His_4 tag was PCR-amplified from fusion protein **b** sequence using forward (5′-ATTCATATGATGGTTTGGAAAAATTTTGGTTACG-3′) and reverse (5′-ATAGCTAGCTTAGTGATGGTGATGGTTCTGTCCTGTTGGAACCAGAG-3′) primers with NdeI and NheI restriction sites, respectively. The amplicons of fusion protein **b** and the catalase-related domain were cloned into the pET11a expression vector (Stratagene) and sequenced. The His-tagged fusion protein **b** and catalase-related domain were expressed in *E. coli* BL21(DE3) cells (Novagen) in a Terrific Broth medium at 20 °C overnight and purified as described previously (17). The protein fractions were dialyzed against an ice-cold 50 mM Tris (pH 8.0) buffer containing 100 mM NaCl by slowly stirring overnight at 4 °C. Purified proteins were stored at −80 °C for further use. Proteins were quantified based on the absorbance at 406 nm ($\epsilon \sim 100{,}000\ M^{-1}\ cm^{-1}$) characteristic for hemoproteins.

*Chiral analysis of C. imbricata Fusion Protein **b**-derived 8-HpETE Intermediate*—Incubations with 5 nM fusion protein **b** were performed at room temperature using 100 μM AA in a 50 mM Tris (pH 8.0) buffer containing 100 mM NaCl and 1 mM $CaCl_2$ in the presence of the reducing agent $SnCl_2$ to reduce the LOX-catalyzed 8-HpETEs *in situ*. Incubations with *Gersemia fruticosa* 8*R*-LOX were performed in parallel. Individual LOX products were extracted with EtOAc, and the corresponding methyl esters were prepared using diazomethane. LOX products were isolated on SP-HPLC using a Phenomenex silica 5-μm column (0.46 × 25 cm) with a hexane/isopropyl alcohol solvent system (isocratic: 100:2 by volume) at a flow rate of 1 ml/min at 235 nm. Methyl esters of 8-HETE were analyzed on a Chiralcel OD-H (0.46 × 25 cm) column at a flow rate of 1 ml/min at 235 nm using the same solvent system as described previously. The methylated *C. imbricata* LOX product was co-chromatographed with the methyl esters of ±8-HETE standard (Cayman Chemical Co.), and the 8*R*-HETE reference by *G. fruticosa* 8*R*-LOX (10) was used to determine the stereoconfiguration of 8-HETE formed by the LOX domain of the *C. imbricata* fusion protein **b**.

*Incubations with Fusion Protein **b** and Catalase-related Domain*—Incubations with 5 nM fusion protein **b** were conducted at room temperature using 100 μM AA in a 50 mM Tris (pH 8.0) buffer containing 100 mM NaCl and 1 mM $CaCl_2$ in a quartz cuvette. The change in the absorbance was recorded by repetitive scanning (200–350 nm) using a Lambda-35 UV-visible spectrometer (PerkinElmer Life Sciences). Alternative substrates, eicosapentaenoic acid (20:5ω3), docosahexaenoic acid (22:6ω3), and 5,8,11-eicosatrienoic acid (20:3ω9) (Cayman Chemical Co.), were tested in parallel. Identical incubations with 5 nM catalase-related domain (the presence of $CaCl_2$ in the incubation is not essential) were performed using 100 μM 8*R*-HpETE as a substrate, and the disappearance of a conjugated diene chromophore ($\epsilon \sim 25{,}000\ M^{-1}\ cm^{-1}$) was recorded at 235 nm. The substrate specificities with 8*RS*-, 11*RS*-, and 11*R*-HpETE were examined in parallel.

To analyze the primary products formed, reactions with 8*R*-HpETE and the catalase-related domain were stopped with the addition of the reducing agent $NaBH_4$ (0.5 mg of $NaBH_4$ per 1 ml of buffer). The reaction was acidified down to pH 4 and loaded on a 1-cc Oasis HLB cartridge (Waters), eluted with 1 ml of MeOH, and stored at −80 °C for further analysis. Products were taken to dryness and dissolved in a corresponding column solvent before the HPLC analyses.

To analyze the oxygen incorporation from the substrate, incubations with 0.3 mM $^{18}O_2$-8*R*-HpETE and 24 μM catalase-related domain were performed in a 1-ml ice-cold incubation buffer either for 30 s or for 2 min on ice. In addition, reactions with 24 μM catalase domain and 2 mM 8*R*-HpETE in a 0.2-ml ice-cold buffer (50 mM Tris (pH 8.0), 100 mM NaCl) containing 0.1 ml $H_2{}^{18}O$ were carried out for 30 s on ice. Control reactions with the unlabeled substrate and water were conducted in parallel. All reactions were stopped by adding $NaBH_4$.

Carbon Monoxide Binding of Ferrous catalase-related Domain—The ferrous state of the catalase-related domain of fusion protein **b** was generated by the addition of sodium dithionite into a 1-ml quartz cuvette containing 1 μM ferric catalase-related domain in the incubation buffer. A ferrous-CO complex was prepared by bubbling CO gas into the cuvette for 2 min. The change in the chromophore of the Soret band (406 nm; ferric cHPL) to a ferrous-CO complex was observed using UV-visible spectrometer scanning at 200–700 nm.

HPLC Analyses—Non-reduced and $NaBH_4$-reduced products were analyzed by RP-HPLC using a C18 Waters Symmetry 5-μm column (46 × 250 mm) with a CH_3CN/H_2O/glacial acetic acid solvent system (gradient: 20:80:0.01 to 80:20:0.01 by

volume for 30 min; isocratic: 80:20:0.01 by volume for 10 min) at a flow rate of 1 ml/min. UV signals at 205, 220, 235, and 270 nm were recorded using an Agilent 1100 series diode array detector. For the ^{1}H NMR analysis, products formed from 2 mg of substrate were extracted on a 6-cc Agilent Bond Elut C18 column and isolated on RP-HPLC using the same solvent system as described previously. Additional purification was performed on SP-HPLC using a Thomson silica 5-μm column (4.6 × 250 mm) with a hexane/isopropyl alcohol/glacial acetic acid column solvent (100:3:0.01 and 100:10:0.01 by volume for polar and less polar compounds, respectively) at a flow rate of 1 ml/min. Isolated products were dissolved in MeOH and stored at −80 °C until further analyses.

RP-HPLC-MS and NMR Analyses—Products formed from 8*R*-HpETE by catalase domain were separated on RP-HPLC using a Kinetex C18 2.6-μm column (3 × 100 mm) with CH_3CN/H_2O/HAc (45:55:0.01, by volume) at 0.4 ml/min, and molecular weights were established from the M-H anions measured by negative ion electrospray LTQ1 iontrap LC-MS instrument.

The products formed from ^{18}O-labeled 8*R*-HpETE by the catalase-related domain were eluted on RP-HPLC/MS using a Kinetex C18 2.6-μm (3 × 100 mm) column with a MeOH/H_2O/HAc solvent system containing 10 mM NH_4OAc, 0.1% AcOH, and 100 μM $AgBF_4$ (gradient: 60:40:0.01 to 90:10:0.01 (MeOH/H_2O/HAc) by volume with a flow rate of 0.2 ml/min for 5 min; isocratic: 90:10:0.01 by volume with a flow rate of 0.3 ml/min). The molecular weights were established from the formed silver adducts using silver coordination on double bonds and the M-H$^+$ cation measured by positive ion electrospray Quantum3 LC-MS instrument.

^{1}H NMR and ^{1}H,^{1}H COSY NMR spectra were recorded on a Bruker 600-MHz spectrometer at 298 K. The parts/million values are reported relative to residual non-deuterated C_6D_6 (δ = 7.16) and $CDCl_3$ (δ = 7.24) for non-reduced and $NaBH_4$-reduced products, respectively. All spectra were analyzed on TopSpin 3.0 software (Bruker).

Results

Heterologous Expression of a Novel Catalase-Lipoxygenase Fusion Protein—The *C. imbricata* catalase-lipoxygenase fusion cDNA including an N-terminal His tag was cloned into the expression vector pET11a, and the 122-kDa protein was expressed in *E. coli* BL21(DE3) with a 1-mg yield of active protein per liter under the conditions described under "Experimental Procedures." The catalase-domain (43 kDa) alone was expressed similarly, obtaining the same yield and activity (Fig. 1). The UV-visible spectrum shows the main Soret band at 406 nm, typical of a high spin ferric catalase (Fig. 1). The absorbance shifted to 427 nm in the CO complex of the dithionite-reduced (ferrous) enzyme, a value close to the reported lambda max of the *P. homomalla* CO complex of ferrous-cAOS (427 nm) (18, 19).

Characterization of the Catalytic Specificity of the LOX Domain—The 8-HpETE formed by *C. imbricata* cHPL-LOX was chromatographed on a Chiralcel OD-H chiral column as the HETE methyl ester derivative as described under "Experimental Procedures." The retention time of the methyl ester of

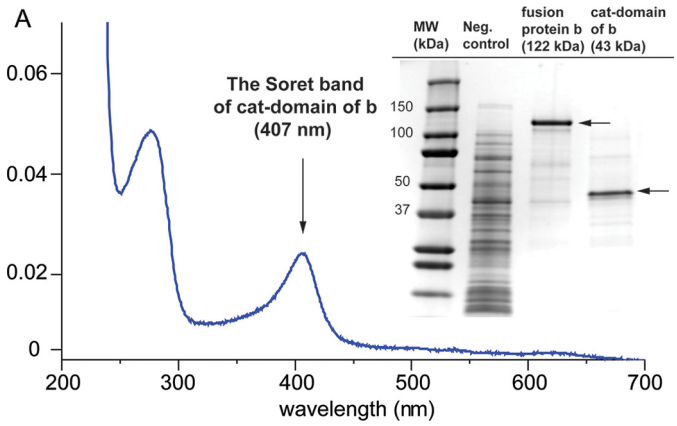

FIGURE 1. **The UV-visible spectrum of catalase-related domain of fusion protein b and the SDS-PAGE gel image of expressed fusion protein b and catalase domain.** *cat-domain of b*, the catalase-related domain of fusion protein **b**.

8-HETE at 15 min corresponds to the 8*R* enantiomer formed by *G. fruticosa* 8*R*-LOX. The chromatogram of the racemic 8-HETE standard analyzed on chiral SP-HPLC appeared in two peaks, the first peak being 8*R* and the second peak 8*S* (10), with retention times at 15 and 18 min, respectively. The methyl ester of 8-HETE co-chromatographed with the racemic 8-HETE standard resulted in an increase of the first peak (data not shown). Therefore, co-elution of the *C. imbricata* fusion protein **b**-derived 8-HETE with the references of 8*R* enantiomer confirms the specificity of the 8*R*-LOX domain.

HPLC Analyses of Products of the Catalase-related Domain—Incubations of 8*R*-HpETE with the His-tagged fusion protein **b** or its catalase-only domain resulted in the disappearance of the conjugated diene chromophore of 8*R*-HpETE and the formation of end products with weak or negligible UV absorbance (Fig. 2). In addition, *C. imbricata* fusion protein **b** converts the substrate analogue 5,8,11-eicosatrienoic acid and naturally occurring eicosapentaenoic acid and docosahexaenoic acid similarly to AA (data not shown). Among arachidonate-derived substrates, the expressed catalase-related domain was specific for 8*R*-HpETE and did not measurably metabolize 8*RS*-HpETE (8*S* being inhibitory) or 11*R*- and 11*RS*-HpETE. The k_{cat} and K_m of cHPL with 8*R*-HpETE were determined as 133 ± 5 s^{-1} and 3.8 ± 0.5 μM, respectively, with a k_{cat}/K_m value of 35 $\mu M^{-1}\,s^{-1}$.

RP-HPLC analysis of the products from 8*R*-HpETE consistently showed the appearance of two very broad UV-205-nm absorbing areas on the chromatogram followed in both cases by a sharp 220-nm peak (Fig. 3*A*). It became apparent (as explained below) that the primary enzymatic products were represented by the exceptionally broad peaks labeled **1** and **2** on Fig. 3*A* and that the sharp peaks labeled **3** and **4** eluting at ~8 and 37 min were actually formed via non-enzymatic isomerization of **1** and **2**, respectively. It was evident at this stage that the catalase domain exhibited a novel activity as no allene oxide-derived α-ketol or cyclopentenone was detected. It was also established that the products were formed by the chain cleavage of 8*R*-HpETE because after incubation and extraction of an incubation of [1-^{14}C]-AA with fusion protein **b**, the ^{14}C label was retained only in the early eluting product **3,** and product **4** was unlabeled (16).

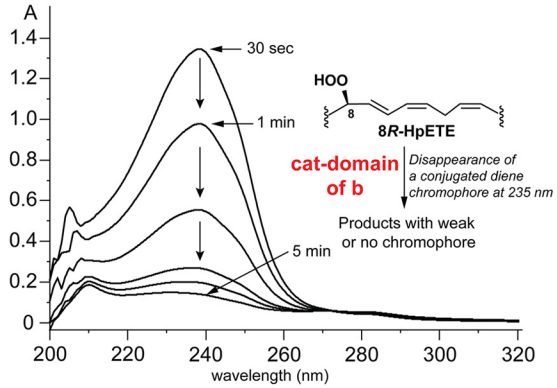

FIGURE 2. **Repetitive UV scans illustrating the transformation of 8*R*-HpETE by the catalase-related domain of *C. imbricata* fusion protein b.** The transformation is associated with the disappearance of the conjugated diene chromophore of 8*R*-HpETE and gives a product(s) with weak or no chromophore. *cat-domain of b*, the catalase-related domain of fusion protein **b**.

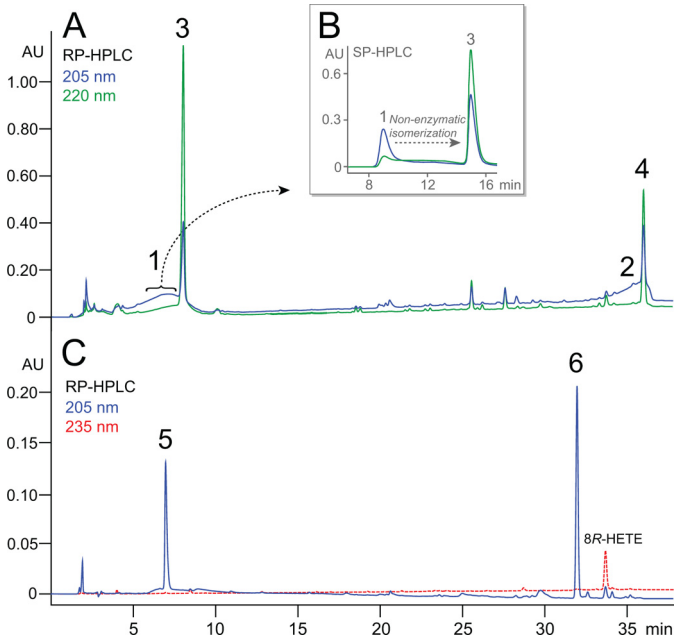

FIGURE 3. **HPLC analyses of products of the catalase domain of b reacting with 8*R*-HpETE.** *A*, RP-HPLC chromatogram of the product profile monitored at 205 nm (*blue line*, showing broad peaks **1** and **2**) and 220 nm (*green line*, sharp peaks of products **3** and **4**). *B*, *inset*, SP-HPLC chromatogram illustrating the non-enzymatic isomerization of isolated product **1** to product **3**. *C*, RP-HPLC chromatogram of the products of *in situ* $NaBH_4$ reduction of the enzymatic incubation, producing **5** and **6** (*blue line*) as alcohol derivatives of products **1** and **2**, respectively, with 8*R*-HETE (reduced substrate) eluting at 34 min and detected at 235 nm (*red line*). The RP-HPLC analyses used a C18 Waters Symmetry 5-μm column (4.6 × 250 mm) at a flow rate of 1 ml/min with a solvent gradient of CH_3CN/H_2O/glacial acetic acid in the proportions 20:80:0.01 to 80:20:0.01 (by volume) over 30 min then held isocratically for 10 min. UV signals at 205, 220, 235, and 270 nm were recorded using an Agilent 1100 series diode array detector. The SP-HPLC in *panel B* used a Thomson silica 5-μm column (4.6 × 250 mm) with hexane/isopropyl alcohol/glacial acetic acid solvent (100:10:0.01, by volume) and a flow rate of 1 ml/min. *AU*, absorbance units.

Once it became apparent that the broad peaks **1** and **2** were a consistent feature of the product profile, product **1** was collected from the initial RP-HPLC run and re-chromatographed on SP-HPLC, (Fig. 3*B*). This clearly showed that product **1** was converting to **3** and, indeed, the elevated baseline between the peaks reflected this transformation in progress (Fig. 3*B*). Initial

TABLE 1

^{1}H NMR chemical shifts (δ) and coupling constants (Hz) of C8-oxo acid (product 3)

NMR analysis was conducted using C_6D_6 solvent.

Hydrogens	Chemical shift (δ)	Coupling constant (Hz)	Multiplicity	Number of protons
H8	9.27	$J_{8,7}$ = 7.6	d	1
H7	5.81	$J_{7,6}$ = 15.6 (trans) $J_{7,8}$ = 7.6	dd	1
H6	5.89	$J_{6,5}$ = 6.5 $J_{6,7}$ = 15.6 (trans)	dt	1
H5	1.52	$J_{5,4}$ = 14.9 $J_{5,6}$ = 7.2	dd	2
H4	0.88	$J_{4,3}$ = 7.8 $J_{4,5}$ = 15.4	m	2
H3	1.18	$J_{3,2}$ = 15.5 $J_{3,4}$ = 7.7	m	2
H2	1.85	$J_{3,4}$ = 14.6	t	2

characterization of the stable products **3** and **4** showed that they each displayed a conjugated enone chromophore (lambda max 225 nm in acetonitrile). The facile isomerization of **1** and **2** would be readily explained by a double bond isomerization to form the conjugated enone systems of **3** and **4**. To prevent this from occurring, an incubation of 8*R*-HpETE with the catalase domain was terminated by the addition of $NaBH_4$ *in situ*, and the resulting products were analyzed by RP-HPLC (Fig. 3*C*); this revealed two new products, designated **5** and **6**, with stable chromatographic characteristics and displaying only 205-nm UV absorbance.

LC-MS and NMR Analyses—Negative ion electrospray LC-MS analysis of product **3** gave an M-1 ion at *m*/*z* 155, corresponding to the predicted mass of an oxo-octenoic acid, whereas product **4** was undetectable. Product **3** was identified by NMR (Table 1). The doublet at 9.27 ppm (H8) represents the C-8 aldehydic proton, which is coupled to H7 at 5.81 ppm with a $J_{5,6}$ coupling of 15.6 Hz to H6 (5.89 ppm) defining the 6,7-trans double bond and the conjugated enone system (Fig. 4*A*). These data and the remaining signals established the structure of **3** as (6*E*)-8-oxo-octenoic acid. Due to volatility and solubility issues, the purification of product **4** for NMR analysis was unsuccessful, and its structure was deduced as the corresponding conjugated C_{12} aldehyde, 1-oxo-2*E*,6*Z*-dodecene, from its UV spectral characteristics and by silver-coordinated LC-MS and NMR analyses of the corresponding C_{12} $NaBH_4$-reduced fragment.

Identification of Products 5 and 6—The $NaBH_4$-reduced products **5** and **6** (Fig. 3*C*) were identified by NMR (Table 2). In the spectrum of product **5** (Table 2, *left*), the triplet at 3.64 ppm had an area of two, representing the geminal C-8 hydrogens, and indicating a primary alcohol. The same applies to the hydroxyl of **6** (H-1 at 3.64 ppm; Table 2, *right*). Most significantly, in each case the primary alcohols were coupled to a CH_2 moiety, which in turn is coupled to a *cis* double bond (10.9 Hz; *cis*); Fig. 4*B*. Together with the rest of the NMR data, the structures of **5** and **6** were thus established as (5*Z*)-8-hydroxy-octenoic acid and (3*Z*,6*Z*)-dodecadien-1-ol, respectively. It follows that the primary products of the catalase domain detected as the broad peaks at 205 nm, products **1** and **2**, were the corresponding aldehydes, (5*Z*)-8-oxo-octenoic acid and (3*Z*,6*Z*)-1-oxo-dodecadienal (Scheme 1). The results establish that the *C. imbricata* catalase domain

of fusion protein **b** displays a novel hydroperoxide lyase activity and that it can be designated as a cHPL, catalase-related hydroperoxide lyase.

Isotopic Analyses of Products Formed by cHPL—Incubations with $^{18}O_2$-labeled 8*R*-HpETE were conducted to define the oxygen incorporation in products and describe the reaction mechanism of cHPL. As aldehydes readily exchange oxygen with water, 30-s incubations with $^{18}O_2$-labeled 8*R*-HpETE and cHPL were conducted on ice, and the primary aldehydes were analyzed after *in situ* reduction with $NaBH_4$ to the corresponding alcohols. The incorporation of ^{18}O in the C8-hydroxy acid and C12-alcohol was determined by LC-MS analyses using a silver coordination methodology that produces ionization of any alkene-containing molecule (20). The two isotopes of silver (107 and 109) were almost equally represented, giving doublets of ions for the silver adducts of (5*Z*)-8-hydroxy acid and (3*Z*,6*Z*)-dodecadien-1-ol at 265/267 and 289/291, respectively, and 267/269 and 291/293 for the corresponding ^{18}O-labeled ions. Additional ions were observed for the ammonium adducts ($[M+18]^+$) with the carboxyl of the C8-hydroxy acid with predicted *m*/*z* for the unlabeled and ^{18}O-labeled species of 176 and 178, respectively.

LC-MS analyses revealed that incubations with ^{18}O-labeled 8*R*-HpETE resulted in the formation of ^{18}O-incorporated C8-hydroxy acid (having *m*/*z* of 267/269, respective to silver adducts, and *m*/*z* of 178, respective to the NH_4^+ adduct) (Fig. 4*C*) and C12-alcohol (*m*/*z* of 291/293 respective to silver adducts) (Fig. 5*D*). The C8-hydroxy acid and C12-alcohol

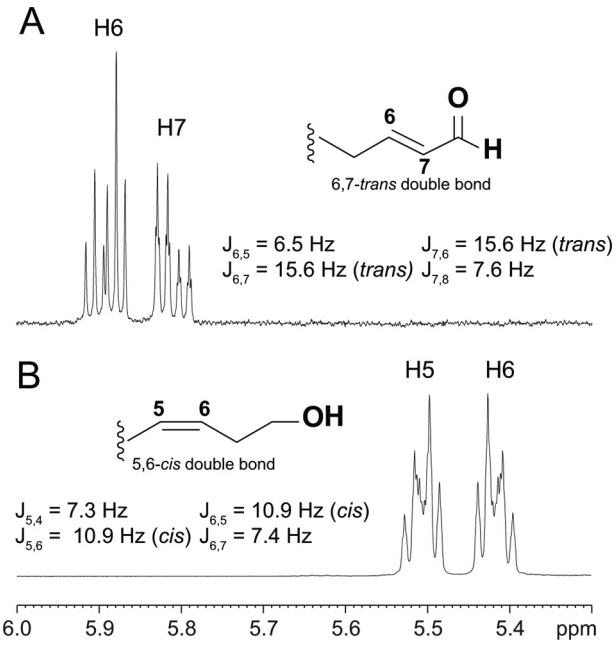

FIGURE 4. **^{1}H NMR one-dimensional spectra of double bond region of (6*E*)-8-oxo-octenoic acid (*A*) and (5*Z*)-8-hydroxy acid (*B*).** Coupling constants between H6 and H7 (*A*) and H5 and H6 (*B*) describe the stereo configuration of the corresponding double bond. The (6*E*)-8-oxo-octenoic acid (*A*) represents isomerized product from primary (6*E*)-8-oxo-octenoic acid, which is analyzed as C8-hydroxy acid derivative (*B*). C8-oxo acid (*A*) and C8-hydroxy acid (*B*) were analyzed in C_6D_6 and $CDCl_3$ solvents, respectively.

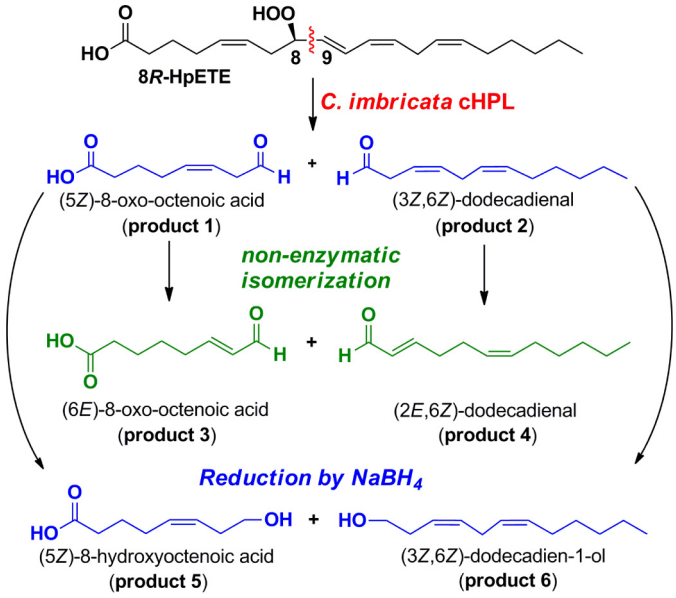

SCHEME 1. **The representation of product formation by cHPL.** Primary products (product **1** and **2**; *blue*) were identified as alcohol derivatives (product **5** and **6**; *blue*). The secondary products (isomerized; product **3** and **4**) are presented as *green*.

TABLE 2

^{1}H NMR chemical shifts (δ) and coupling constants (Hz) of C12-hydroxy acid (left) and C12-alcohol (right)

NMR analysis was conducted using a $CDCl_3$ solvent (left and right).

C8-hydroxy acid (product 5)					C12 alcohol (product 6)				
Hydrogens	Chemical shift (δ)	Coupling constant (Hz)	Multiplicity	Number of protons	Hydrogens	Chemical shift (δ)	Coupling constant (Hz)	Multiplicity	Number of protons
H8	3.64	$J_{8,7}$ = 12.9	t	2	H12	0.87	$J_{12,11}$ = 6.7	t	3
H7	2.31	$J_{7,6}$ = 6.8 $J_{7,8}$ = 13.2	q	2	H9	1.35	$J_{9,8}$ = 7.1 $J_{9,10}$ = 10.6	m	2
H6	5.42	$J_{6,5}$ = 10.9 (cis) $J_{6,7}$ = 7.4	m	1	H8	2.03	$J_{8,7}$ = 7.3 $J_{8,9}$ = 7.2	q	2
H5	5.51	$J_{5,4}$ = 7.3 $J_{5,6}$ = 10.9 (cis)	m	1	H7	5.38	$J_{7,6}$ = 10.9 (cis) $J_{7,8}$ = 7.3	m	1
H4	2.13	$J_{4,3}$ = 14.6 $J_{4,5}$ = 7.3	q	2	H6	5.31	$J_{6,7}$ = 10.6 (cis) $J_{6,5}$ = 7.1	dt	1
H3	1.71	$J_{3,2}$ = 7.3 $J_{3,4}$ = 14.7	m	2	H5	2.81	$J_{5,6}$ = 7.3 $J_{5,4}$ = 7.3	t	2
H2	2.35	$J_{3,2}$ = 14.6	t	2	H4	5.52	$J_{4,5}$ = 7.4 $J_{4,3}$ = 10.7 (cis)	dt	1
					H3	5.38	$J_{3,4}$ = 10.7 (cis) $J_{3,2}$ = 7.3	m	1
					H2	2.43	$J_{2,1}$ = 13.4 $J_{2,3}$ = 6.8	q	2
					H1	3.64	$J_{1,2}$ = 6.5	t	2

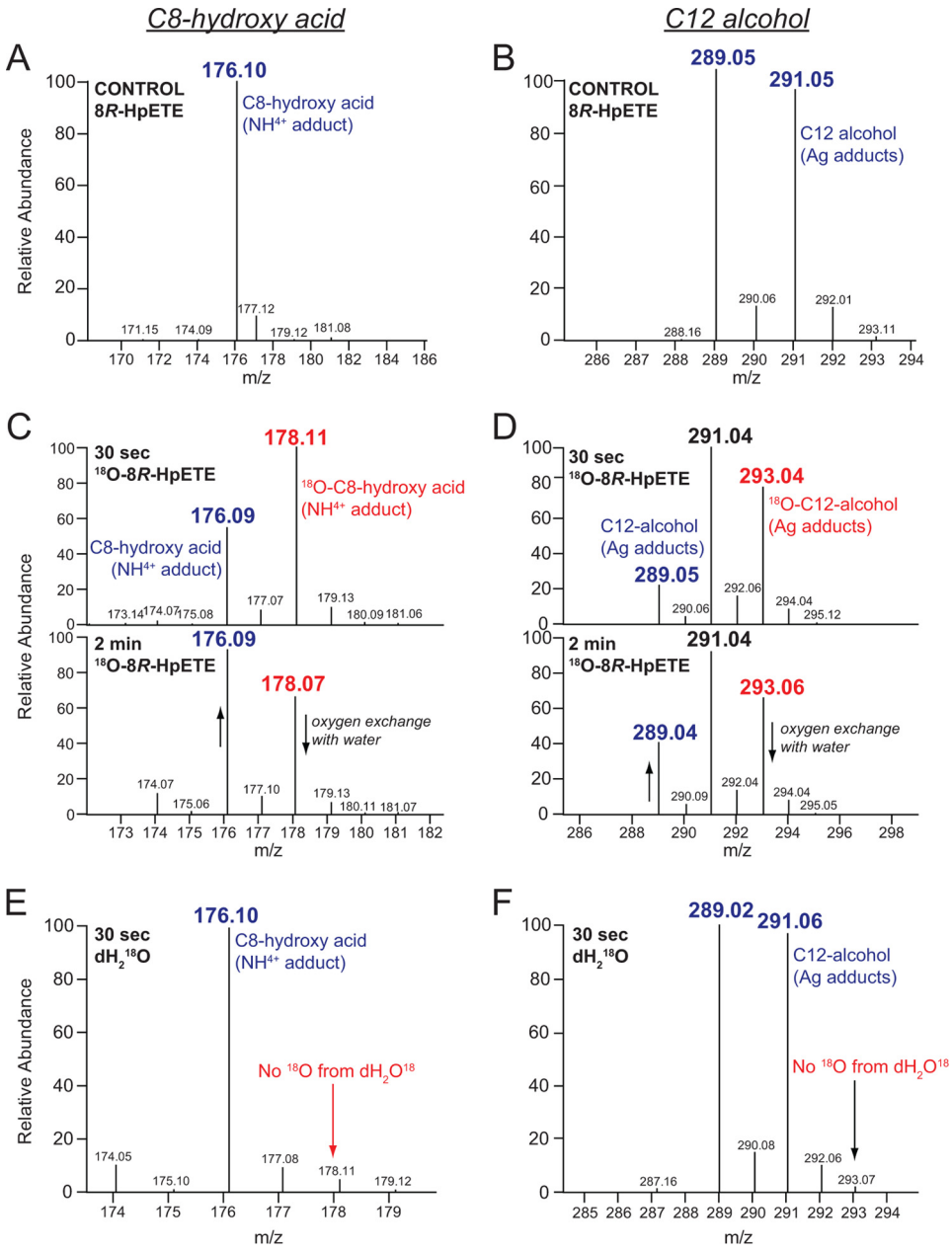

FIGURE 5. **LC-MS analysis of ^{18}O incorporation in the $NaBH_4$-reduced products of *C. imbricata* cHPL.** The *left panels* illustrate the NH_4^+ adduct ions of the C8-hydroxy acid (*panels A*, *C*, and *E*) and the *right panels* show the doublet of Ag^+ adduct ions of the C12 alcohol (*panels B*, *D*, and *F*). *A* and *B*, the ion profiles from 30-s incubation of cHPL with unlabeled 8*R*-HpETE. *C* and *D*, after incubation of cHPL with [$^{18}O_2$]8*R*-HpETE for 30 s or 2 min, illustrating ^{18}O incorporation and the partial loss of ^{18}O in the 2 min incubation. *E* and *F*, the ion profiles from the incubation of cHPL with unlabeled 8*R*-HpETE in the presence of ^{18}O-labeled water. For clarity, only NH_4^+ adducts of the C8-hydroxy acid are shown. The ^{16}O- and ^{18}O-containing products are presented as *blue* and *red*, respectively.

formed in a $H_2{}^{18}O$-containing buffer (Fig. 5, *E* and *F*, respectively) did not contain any oxygen-18 isotope and were identical to the control incubations (Fig. 5, *A* and *B*, respectively). The altered ratios of ^{16}O and ^{18}O in C8-hydroxy acid and C12-alcohol after longer incubation (2 min instead of 30 s) illustrate the time dependence in oxygen exchange between the aldehydes and water (Figs. 5*C* and 4*D*). These results establish that the hydroperoxy oxygens of 8*R*-HpETE are retained in the two aldehydic fragments, a mechanism consistent with the conversion of 8*R*-HpETE to a hemiacetal derivative that spontaneously breaks down to the two-chain cleavage products (21).

Discussion

Currently, although individual lipoxygenases have been described in corals (22–25), only 8*R*-LOX seems to be associated with a catalase-related/LOX fusion protein (9, 10, 16). The structural analysis of the *P. homomalla* cAOS domain of the cAOS-LOX fusion protein revealed that conservation of the catalase core structure (14) and the most significant catalase-related residues are also present in cHPL, thus expanding the diversity of heme-containing catalase-related enzymes in the fatty acid hydroperoxide metabolism. Illustrating the independence of both domains, the separately

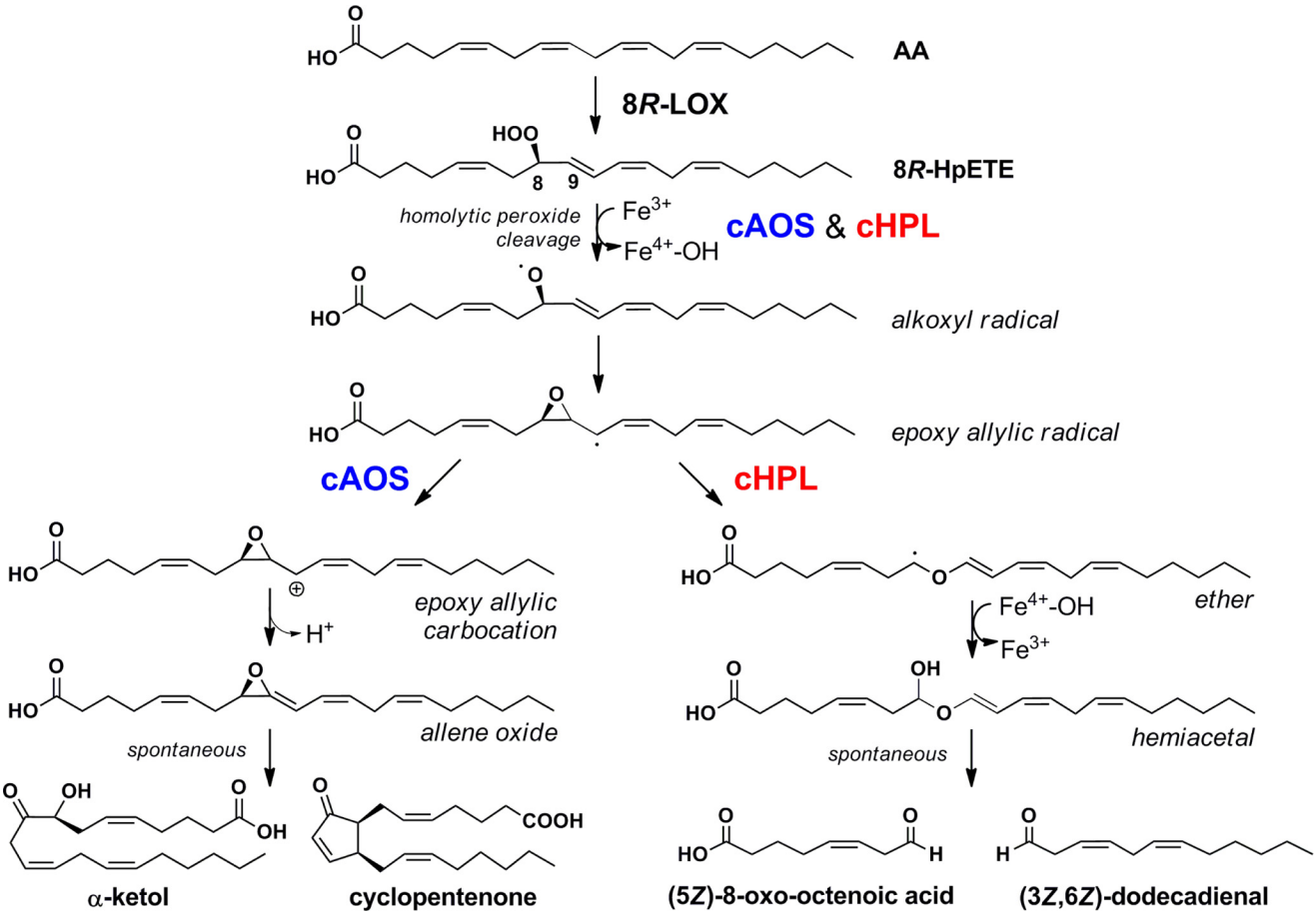

SCHEME 2. **The cAOS (*left*) and cHPL (*right*) pathways in soft coral *C. imbricata*.**

expressed *P. homomalla* AOS-LOX domains each retained activity (11), and a similar functional independence of the two domains of the cHPL-LOX was shown here. The covalent linkage of cHPL with 8*R*-LOX probably helps to target the fusion protein into membranes, assuring the close proximity of the component domains to the newly released arachidonic acid substrate, as demonstrated with cAOS-LOX (26).

We determined the catalytic efficiency (k_{cat}/K_m) of the *C. imbricata* cHPL as 35 μM^{-1} s^{-1}, which is similar to the *P. homomalla* cAOS, 31 μM^{-1} s^{-1} (11). The catalytic efficiency of the plant cytochrome P450 HPL (CYP74) can be highly variable, depending on the inclusion of detergents. For example, for a *Medicago truncatula* CYP74 HPL with its optimal substrate 13*S*-hydroperoxy-C18:3ω3, the k_{cat}/K_m varied from 3 to 151 μM^{-1} s^{-1} in the presence and absence of detergent, respectively (27). Although the enzymatic efficiency of HPLs are comparable, the turnover numbers reported for the CYP74 HPLs are an order of magnitude higher than for the *C. imbricata* cHPL (28–31).

Reaction Mechanism of cHPL—Our evidence indicates that the coral cHPL catalyzes the C8-oxo acid and C12-aldehyde formation from 8*R*-HpETE in a route precedented for cytochrome P450 HPL enzymes. It is generally agreed that plant P450 CYP74 family enzymes homolytically cleave the fatty acid hydroperoxide moiety to form an epoxyallylic carbon radical intermediate from which a number of biosynthetic outcomes are known (3). These include allene oxide synthase and divinyl ether synthase transformations (2, 3, 32). In the third possibility, the HPL route, the rearrangement leads to a covalently complete yet unstable final product, a full-length fatty acid hemiacetal, which through spontaneous decomposition gives the two short-chain aldehydic products (21, 33). The equivalent pathway for the coral cHPL is illustrated in Scheme 2. The ferric cHPL enzyme catalyzes a homolytic cleavage of the 8*R*-hydroperoxy group with oxidation of the heme to Compound II (Fe^{4+}-OH). The fatty acid alkoxyl radical cyclizes to an epoxy allylic radical. At this point the steps promoted by cAOS or cHPL diverge. cAOS stabilizes the carbocation formation and catalyzes the hydrogen abstraction, which results in the formation of allene oxide (Scheme 2, *left side*). cHPL stabilizes the epoxy allylic radical and initiates the cleavage of C8-C9-bond in the epoxy group, which results in an allylic ether radical formation. The oxygen rebound from Compound II gives rise to a hemiacetal intermediate. Our isotopic analysis and results by Grechkin and co-workers (21, 33) clearly demonstrate that water is not involved in this process and that both of the original hydroperoxide oxygens are retained in the products. Notably, the chain cleavage in the P450 and cHPL type of fatty acid hydroperoxide lyase occurs within the original pentadiene of the fatty acid hydroperoxide, between C8 and C9 in the case of coral cHPL.

Technical Challenges in the HPLC Analysis of 3Z-Aldehydes—In our study we observed exceptionally adverse chromatographic behavior of the two primary cHPL products,

each containing an aldehydic moiety with a 3*Z* double bond. On RP-HPLC each primary product ran as an abnormal broad band rather than as a distinct peak (Fig. 3), and poor performance was observed also on SP-HPLC (Fig. 3*B*). Although we could attribute this anomalous performance partly to isomerization to the conjugated enal (the corresponding 2*E*-aldehydic isomer), our impression is that this is not the only issue. The broad bands on RP-HPLC do not show the characteristic enal chromophore of the 2*E*-aldehydes, suggesting that some adverse interaction of the 3*Z*-aldehydes occurs with the HPLC solvent and stationary phase. One of us has prior experience with the HPLC of an authentic sample of a plant CYP74B lyase product (3*Z*-nonenal) (31), and the same phenomenon was evident, suggesting it is general to the 3*Z*-aldehydes. As volatile molecules, 3*Z*-aldehydes are commonly detected among short-chain fragments of fatty acids, and there is very substantial literature on their analysis. However, the chromatographic analyses are typically restricted to gas chromatography in which the chromatographic behavior is quite normal. To the best of our knowledge the adverse HPLC characteristics of the 3*Z*-aldehydes have not been generally recognized or reported.

A Contrasting Route to Fatty Acid Chain Cleavage—The coral cHPL is unique in the animal kingdom. The mechanism and products of transformation are distinct from unrelated enzymatic and non-enzymatic lyase reactions that produce chain cleavage between the hydroperoxide-bearing carbon and the CH_2 moiety in the α position outside the original pentadiene. To give an example of the latter involving the identical fatty acid hydroperoxide substrate, 8*R*-HpETE, whereas cHPL gives rise to C8 and C12 aldehydes, there is an uncharacterized lyase activity in starfish oocytes that cleaves the carbon chain between C7 and C8, producing a C7-aldehyde acid and C13 aldehyde (34). Non-enzymatic transformation by free heme favors a similar pathway (*e.g.* Refs. 35 and 36). This alternative type of lyase reaction is known to be initiated by LOX enzymes and is facilitated under anaerobic conditions (37, 38). Examples include the reactions of porcine leukocyte 12-LOX (39) and rabbit leukocytes (40) and the lipoxygenase-lyase pathway in the moss *Physcomitrella patens* (41).

Biological Significance of HPL Metabolism—The AA-derived C8-oxo acid and C12-aldehyde with their isomerized derivatives are potential biologically active signal mediators in corals. In plants, the HPL-derived green leaf volatiles are shown as mediators in abiotic and biotic stress (42). The (3*Z*)-hexenal and 12-oxo-*cis*-dodecenoic acid formed by 13-HPL have the capability to isomerize non-enzymatically (43) or by the isomerases (44, 45) to biologically active forms, 2*E*-hexenal and 12-oxo-trans-dodecenoic acid (also known as traumatin), respectively. Traumatin plays an important role in plant wound healing (46), and 2(*E*)-hexenal induces the expression of HPL, AOS, LOX (47, 48), and other stress genes in plants (49). Moreover, the electrophilic α,β-unsaturated carbonyl group of aldehydes might interact with nucleophiles in biological systems (50, 51), and in plants, antimicrobial properties of oxylipins including 2(*E*)-hexenal have been presented by Prost *et al.* (52).

As mentioned in the Introduction, our previous studies detected what we termed the "unknown polar compounds" in *C. imbricata* that were identified here as aldehydic products of the cHPL-LOX. These products and the gene expression of the cHPL-LOX were measureable in coral samples under baseline conditions and after wounding (16) and thermal-induced stress (a change in sea water temperature from 23 °C to 28 °C or 31 °C) (53). In contrast to the increased gene expression of the cAOS-LOX fusion protein induced both by wounding and thermal stress, the gene expression of the cHPL-LOX was stable during these test conditions. There are few possible interpretations of this apparent lack of enhancement of the cHPL-LOX activity; (i) in contrast to its plant counterpart, the cHPL may not be involved in a response to mechanical injury, and (ii) given that plant oxylipin synthesis is activated within seconds or a few minutes of wounding (54, 55), a short-lived increase in the cHPL-LOX products may occur immediately after wounding, which has not been analyzed (16, 53). Activation of the plant HPL pathway is associated with changes in the expression of other defense genes (47, 49, 56), and equivalent experiments to explore effects of the coral lyase products are required to elucidate the role of cHPL-LOX pathway.

Author Contributions—T. T., H. L., A. R. B., and N. S. designed the study and wrote the paper. H. L. and T. T. cloned the constructs, and T. T. performed the experiments. MS experiments and analysis were conducted by T. T. and W. M. C. NMR analysis was conducted by T. T. and W. E. B. All authors reviewed the results and approved the final version of the manuscript.

References

1. Tanabe, T., and Ullrich, V. (1995) Prostacyclin and thromboxane synthases. *J. Lipid Mediat. Cell Signal.* **12,** 243–255
2. Grechkin, A. N. (2002) Hydroperoxide lyase and divinyl ether synthase. *Prostaglandins Other Lipid Mediat.* **68,** 457–470
3. Brash, A. R. (2009) Mechanistic aspects of CYP74 allene oxide synthases and related cytochrome P450 enzymes. *Phytochemistry* **70,** 1522–1531
4. Feussner, I., and Wasternack, C. (2002) The lipoxygenase pathway. *Annu. Rev. Plant Biol.* **53,** 275–297
5. Garscha, U., Jernerén, F., Chung, D., Keller, N. P., Hamberg, M., and Oliw, E. H. (2007) Identification of dioxygenases required for *Aspergillus* development: studies of products, stereochemistry, and the reaction mechanism. *J. Biol. Chem.* **282,** 34707–34718
6. Hoffmann, I., Jernerén, F., and Oliw, E. H. (2013) Expression of fusion proteins of *Aspergillus terreus* reveals a novel allene oxide synthase. *J. Biol. Chem.* **288,** 11459–11469
7. Brodhun, F., and Feussner, I. (2011) Oxylipins in fungi. *FEBS J.* **278,** 1047–1063
8. Tsitsigiannis, D. I., and Keller, N. P. (2007) Oxylipins as developmental and host-fungal communication signals. *Trends Microbiol.* **15,** 109–118
9. Koljak, R., Boutaud, O., Shieh, B. H., Samel, N., and Brash, A. R. (1997) Identification of a naturally occurring peroxidase-lipoxygenase fusion protein. *Science* **277,** 1994–1996
10. Lõhelaid, H., Järving, R., Valmsen, K., Varvas, K., Kreen, M., Järving, I., and Samel, N. (2008) Identification of a functional allene oxide synthase-lipoxygenase fusion protein in the soft coral *Gersemia fruticosa* suggests the generality of this pathway in octocorals. *Biochim. Biophys. Acta* **1780,** 315–321
11. Boutaud, O., and Brash, A. R. (1999) Purification and catalytic activities of the two domains of the allene oxide synthase-lipoxygenase fusion protein of the coral *Plexaura homomalla*. *J. Biol. Chem.* **274,** 33764–33770
12. Lee, D. S., Nioche, P., Hamberg, M., and Raman, C. S. (2008) Structural insights into the evolutionary paths of oxylipin biosynthetic enzymes. *Nature* **455,** 363–368
13. Li, L., Chang, Z., Pan, Z., Fu, Z. Q., and Wang, X. (2008) Modes of heme binding and substrate access for cytochrome P450 CYP74A revealed by

crystal structures of allene oxide synthase. *Proc. Natl. Acad. Sci. U.S.A.* **105,** 13883–13888
14. Oldham, M. L., Brash, A. R., and Newcomer, M. E. (2005) The structure of coral allene oxide synthase reveals a catalase adapted for metabolism of a fatty acid hydroperoxide. *Proc. Natl. Acad. Sci. U.S.A.* **102,** 297–302
15. Tosha, T., Uchida, T., Brash, A. R., and Kitagawa, T. (2006) On the relationship of coral allene oxide synthase to catalase: a single active site mutation that induces catalase activity in coral allene oxide synthase. *J. Biol. Chem.* **281,** 12610–12617
16. Lõhelaid, H., Teder, T., Tõldsepp, K., Ekins, M., and Samel, N. (2014) Up-regulated expression of AOS-LOXa and increased eicosanoid synthesis in response to coral wounding. *PloS ONE* **9,** e89215
17. Brash, A. R., Niraula, N. P., Boeglin, W. E., and Mashhadi, Z. (2014) An ancient relative of cyclooxygenase in cyanobacteria is a linoleate 10*S*-dioxygenase that works in tandem with a catalase-related protein with specific 10*S*-hydroperoxide lyase activity. *J. Biol. Chem.* **289,** 13101–13111
18. Abraham, B. D., Sono, M., Boutaud, O., Shriner, A., Dawson, J. H., Brash, A. R., and Gaffney, B. J. (2001) Characterization of the coral allene oxide synthase active site with UV-visible absorption, magnetic circular dichroism, and electron paramagnetic resonance spectroscopy: evidence for tyrosinate ligation to the ferric enzyme heme iron. *Biochemistry* **40,** 2251–2259
19. Bandara, D. M., Sono, M., Bruce, G. S., Brash, A. R., and Dawson, J. H. (2011) Coordination modes of tyrosinate-ligated catalase-type heme enzymes: magnetic circular dichroism studies of *Plexaura homomalla* allene oxide synthase, *Mycobacterium avium* ssp. paratuberculosis protein-2744c, and bovine liver catalase in their ferric and ferrous states. *J. Inorg. Biochem.* **105,** 1786–1794
20. Havrilla, M. C., and Hachey, D. L. P., N. A. (2000) Coordination (Ag^+) ion spray-mass spectrometry of peroxidation products of cholesterol linoleate and cholesterol arachidonate: high-performance liquid chromatography-mass spectrometry analysis of peroxide products from polyunsaturated lipid autoxidation. *J. Am. Chem. Soc.* **122,** 8042–8055
21. Grechkin, A. N., and Hamberg, M. (2004) The "heterolytic hydroperoxide lyase" is an isomerase producing a short-lived fatty acid hemiacetal. *Biochim. Biophys. Acta* **1636,** 47–58
22. Eek, P., Järving, R., Järving, I., Gilbert, N. C., Newcomer, M. E., and Samel, N. (2012) Structure of a calcium-dependent 11*R*-lipoxygenase suggests a mechanism for Ca^{2+} regulation. *J. Biol. Chem.* **287,** 22377–22386
23. Mortimer, M., Järving, R., Brash, A. R., Samel, N., and Järving, I. (2006) Identification and characterization of an arachidonate 11*R*-lipoxygenase. *Arch. Biochem. Biophys.* **445,** 147–155
24. Järving, R., Lõokene, A., Kurg, R., Siimon, L., Järving, I., and Samel, N. (2012) Activation of 11*R*-lipoxygenase is fully Ca^{2+}-dependent and controlled by the phospholipid composition of the target membrane. *Biochemistry* **51,** 3310–3320
25. Brash, A. R., Boeglin, W. E., Chang, M. S., and Shieh, B. H. (1996) Purification and molecular cloning of an 8*R*-lipoxygenase from the coral *Plexaura homomalla* reveal the related primary structures of *R*- and *S*-lipoxygenases. *J. Biol. Chem.* **271,** 20949–20957
26. Gilbert, N. C., Niebuhr, M., Tsuruta, H., Bordelon, T., Ridderbusch, O., Dassey, A., Brash, A. R., Bartlett, S. G., and Newcomer, M. E. (2008) A covalent linker allows for membrane targeting of an oxylipin biosynthetic complex. *Biochemistry* **47,** 10665–10676
27. Hughes, R. K., Yousafzai, F. K., Ashton, R., Chechetkin, I. R., Fairhurst, S. A., Hamberg, M., and Casey, R. (2008) Evidence for communality in the primary determinants of CYP74 catalysis and of structural similarities between CYP74 and classical mammalian P450 enzymes. *Proteins* **72,** 1199–1211
28. Noordermeer, M. A., Van Dijken, A. J., Smeekens, S. C., Veldink, G. A., and Vliegenthart, J. F. (2000) Characterization of three cloned and expressed 13-hydroperoxide lyase isoenzymes from alfalfa with unusual N-terminal sequences and different enzyme kinetics. *Eur. J. Biochem.* **267,** 2473–2482
29. Matsui, K., Ujita, C., Fujimoto, S., Wilkinson, J., Hiatt, B., Knauf, V., Kajiwara, T., and Feussner, I. (2000) Fatty acid 9- and 13-hydroperoxide lyases from cucumber. *FEBS Lett.* **481,** 183–188
30. Matsui, K., Miyahara, C., Wilkinson, J., Hiatt, B., Knauf, V., and Kajiwara, T. (2000) Fatty acid hydroperoxide lyase in tomato fruits: cloning and properties of a recombinant enzyme expressed in *Escherichia coli*. *Biosci. Biotechnol. Biochem.* **64,** 1189–1196
31. Tijet, N., Schneider, C., Muller, B. L., and Brash, A. R. (2001) Biogenesis of volatile aldehydes from fatty acid hydroperoxides: molecular cloning of a hydroperoxide lyase (CYP74C) with specificity for both the 9- and 13-hydroperoxides of linoleic and linolenic acids. *Arch. Biochem. Biophys.* **386,** 281–289
32. Hamberg, M. (1989) Fatty acid allene oxides. *J. Am. Oil Chem. Soc.* **66,** 1445–1449
33. Grechkin, A. N., Brühlmann, F., Mukhtarova, L. S., Gogolev, Y. V., and Hamberg, M. (2006) Hydroperoxide lyases (CYP74C and CYP74B) catalyze the homolytic isomerization of fatty acid hydroperoxides into hemiacetals. *Biochim. Biophys. Acta* **1761,** 1419–1428
34. Brash, A. R., Hughes, M. A., Hawkins, D. J., Boeglin, W. E., Song, W. C., and Meijer, L. (1991) Allene oxide and aldehyde biosynthesis in starfish oocytes. *J. Biol. Chem.* **266,** 22926–22931
35. Gardner, H. W. (1989) Oxygen radical chemistry of polyunsaturated fatty acids. *Free Radic. Biol. Med.* **7,** 65–86
36. Labeque, R., and Marnett, L. J. (1988) Reaction of hematin with allylic fatty acid hydroperoxides: identification of products and implications for pathways of hydroperoxide-dependent epoxidation of 7,8-dihydroxy-7,8-dihydrobenzo[a]pyrene. *Biochemistry* **27,** 7060–7070
37. Garssen, G. J., Vliegenthart, J. F., and Boldingh, J. (1971) An anaerobic reaction between lipoxygenase, linoleic acid, and its hydroperoxides. *Biochem. J.* **122,** 327–332
38. Garssen, G. J., Vliegenthart, J. F., and Boldingh, J. (1972) The origin and structures of dimeric fatty acids from the anaerobic reaction between soya-bean lipoxygenase, linoleic acid, and its hydroperoxide. *Biochem. J.* **130,** 435–442
39. Glasgow, W. C., Harris, T. M., and Brash, A. R. (1986) A short-chain aldehyde is a major lipoxygenase product in arachidonic acid-stimulated porcine leukocytes. *J. Biol. Chem.* **261,** 200–204
40. Lam, B. K., Linh, Y. L., Ho, H. Y., and Wong, P. Y. (1987) Hydroperoxide lyase in rabbit leukocytes: conversion of 15-hydroperoxyeicosatetraenoic acid to 15-keto-pentadeca-5,8,11,13-tetraenoic acid. *Biochem. Biophys. Res. Commun.* **149,** 1111–1117
41. Wichard, T., Göbel, C., Feussner, I., and Pohnert, G. (2004) Unprecedented lipoxygenase/hydroperoxide lyase pathways in the moss *Physcomitrella patens*. *Angew. Chem. Int. Ed. Engl.* **44,** 158–161
42. Matsui, K. (2006) Green leaf volatiles: hydroperoxide lyase pathway of oxylipin metabolism. *Curr. Opin. Plant Biol.* **9,** 274–280
43. Noordermeer, M. A., Van Der Goot, W., Van Kooij, A. J., Veldsink, J. W., Veldink, G. A., and Vliegenthart, J. F. (2002) Development of a biocatalytic process for the production of C6-aldehydes from vegetable oils by soybean lipoxygenase and recombinant hydroperoxide lyase. *J. Agric. Food Chem.* **50,** 4270–4274
44. Noordermeer, M. A., Veldink, G. A., and Vliegenthart, J. F. (1999) Alfalfa contains substantial 9-hydroperoxide lyase activity and a 3*Z*:2*E*-enal isomerase. *FEBS Lett.* **443,** 201–204
45. Takamura, H., and Gardner, H. W. (1996) Oxygenation of (3*Z*)-alkenal to (2*E*)-4-hydroxy-2-alkenal in soybean seed (*Glycine max* L.). *Biochim. Biophys. Acta* **1303,** 83–91
46. Zimmerman, D. C., and Coudron, C. A. (1979) Identification of traumatin, a wound hormone, as 12-oxo-trans-10-dodecenoic acid. *Plant Physiol.* **63,** 536–541
47. Bate, N. J., and Rothstein, S. J. (1998) C6-volatiles derived from the lipoxygenase pathway induce a subset of defense-related genes. *Plant J.* **16,** 561–569
48. Gomi, K., Yamasaki, Y., Yamamoto, H., and Akimitsu, K. (2003) Characterization of a hydroperoxide lyase gene and effect of C6-volatiles on expression of genes of the oxylipin metabolism in citrus. *J. Plant Physiol.* **160,** 1219–1231
49. Kishimoto, K., Matsui, K., Ozawa, R., and Takabayashi, J. (2005) Volatile C6-aldehydes and Allo-ocimene activate defense genes and induce resistance against *Botrytis cinerea* in *Arabidopsis thaliana*. *Plant Cell Physiol.* **46,** 1093–1102
50. Farmer, E. E., and Davoine, C. (2007) Reactive electrophile species. *Curr. Opin. Plant Biol.* **10,** 380–386

51. Mueller, M. J., and Berger, S. (2009) Reactive electrophilic oxylipins: pattern recognition and signalling. *Phytochemistry* **70,** 1511–1521
52. Prost, I., Dhondt, S., Rothe, G., Vicente, J., Rodriguez, M. J., Kift, N., Carbonne, F., Griffiths, G., Esquerré-Tugayé, M. T., Rosahl, S., Castresana, C., Hamberg, M., and Fournier, J. (2005) Evaluation of the antimicrobial activities of plant oxylipins supports their involvement in defense against pathogens. *Plant Physiol.* **139,** 1902–1913
53. Lõhelaid, H., Teder, T., and Samel, N. (2015) Lipoxygenase-allene oxide synthase pathway in octocoral thermal stress response. *Coral Reefs* **34,** 143–154
54. D'Auria, J. C., Pichersky, E., Schaub, A., Hansel, A., and Gershenzon, J. (2007) Characterization of a BAHD acyltransferase responsible for producing the green leaf volatile (Z)-3-hexen-1-yl acetate in *Arabidopsis thaliana*. *Plant J.* **49,** 194–207
55. Glauser, G., Dubugnon, L., Mousavi, S. A., Rudaz, S., Wolfender, J. L., and Farmer, E. E. (2009) Velocity estimates for signal propagation leading to systemic jasmonic acid accumulation in wounded *Arabidopsis*. *J. Biol. Chem.* **284,** 34506–34513
56. Bate, N. J., Sivasankar, S., Moxon, C., Riley, J. M., Thompson, J. E., and Rothstein, S. J. (1998) Molecular characterization of an *Arabidopsis* gene encoding hydroperoxide lyase, a cytochrome P-450 that is wound inducible. *Plant Physiol.* **117,** 1393–1400